Low Temperature Chemical Precipitation and Characterization of Ceria Based Ceramic Composite Oxide Materials

Devi RADHIKA and A. Samson NESARAJ*

Department of Chemistry, Karunya University, Coimbatore - 641 114, Tamil Nadu, India

Abstract

Ceria based ceramic composite oxide materials such as $Ce_{0.9}Gd_{0.1}O_{2-\delta}$ -$Ce_{0.9}Y_{0.1}O_{2-\delta}$ and $Ce_{0.8}Gd_{0.2}O_{2-\delta}$-$Ce_{0.8}Y_{0.2}O_{2-\delta}$ were prepared by a simple chemical precipitation method for application in low temperature solid oxide fuel cells (LTSOFCs) as electrolytes. The precursor materials used in this synthesis were cerium nitrate hexahydrate, gadolinium nitrate and yttrium nitrate (as basic materials), sodium hydroxide (as precipitator material) and PVA (as surfactant). A mixture of metal hydroxides was formed when the aqueous mixture of basic materials mixed with the aqueous precipitant solution in proper stoichiometric composition. The resultant hydroxide mixture was washed with ethanol and water mixture (1:9 volume ratio) to remove any unwanted impurities present along with the precipitate. The purified precipitate was dried at 50-100°C and heat treated at 300°C, 450°C, 600°C and 750°C for 2 h each to get phase pure ceramic composite oxide materials. The resultant ceramic composite oxide materials were characterized by XRD, FT-IR, particle size analysis and SEM techniques. From the results, it was found that the chemical precipitation can be used effectively to prepare phase pure ceria based ceramic composite oxide materials.

Keywords: Ceria based ceramic composite oxides; Chemical precipitation; Characterization

Introduction

Solid oxide fuel cells (SOFCs) offer an environmentally friendly technology to convert gaseous fuels such as hydrogen, natural gas or gasified coal into electricity at high efficiencies. Besides the higher efficiency than those obtained from the traditional energy conversion systems, a fuel cell provides many other advantages like reliability, modularity, fuel flexibility and very low levels of NO_x and SO_x emissions. The SOFC performance strongly depends on the morphology and composition of the electrodes and electrolytes [1]. Low Temperature SOFC (LTSOFC) is a new trend in SOFC technology, and High Temperature SOFC (HTSOFC) puts very high demands on the materials, and becomes too expensive to match marketability. As one of the most reactive rare earth oxides, ceria, and ceria-based materials play important roles in various applications such as catalysts and in SOFC systems [2, 3]. Because of their high ionic conductivity at relatively moderate temperatures (above 600°C), these materials have potential applications in electrolytes for SOFCs at intermediate temperatures [4-8]. These materials demonstrate much higher ionic conductivity atrelatively lower temperatures in comparison to that of the traditional electrolyte yttria-stabilized zirconia (YSZ). So far, many studies have been carried out on doped ceria and made much progress [9-11]. A wide variety of chemical routes are available for the synthesis of mixed oxide ceramic powders. Doped ceria powder has been reported to be synthesized by various wet chemical routes, such as co-precipitation [12], hydrothermal [13], sol-gel [14], salt-assisted aerosol decomposition [15] and solution combustion route [16]. Further, it has been reported that some singly doped ceria based electrolytes, such as $Ce_{1-x}Gd_xO_{2-\delta}$ (GDC), $Ce_{1-x}Sm_xO_{2-\delta}$ (SDC) and $Ce_{1-x}Y_xO_{2-\delta}$ (YDC) show high oxide ion conductivity. However, the SOFCs based on those have not met the commercial requirement up to now. With the purpose of further optimize electrolyte, co-doping method has been used in recent years and was proved to be effective. Co-doping with an appropriate ratio of Gd^{3+} and Y^{3+} can effectively improve the ionic conductivity of ceria-based electrolytes [17-18]. Up to now, however little work has been carried out on the synthesis of doped ceria based ceramic composite powder using co-doping process. Among the various techniques reported, co-precipitation technique is a simple and promising process to produce homogeneous and

* Corresponding author Email: drsamson@karunya.edu

small-sized powders. It is well known that in soft chemical synthesis, surfactant addition has an important effect on the solution and micro structure of the resultant. Poly(vinyl alcohol) (PVA) can be an effective surfactant especially to avoid agglomeration during the synthesis of nanoceramic powders [19-22]. In this study, homogeneous composite powders of GDC-YDC were synthesized by the hydroxide co-precipitation method with and without addition of surfactant (PVA). The physical properties of the prepared powders (after the heat treatment at 750°C for 2 h) were investigated and the comparative results were presented in this research article.
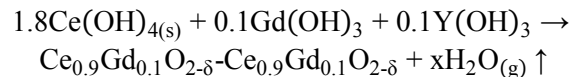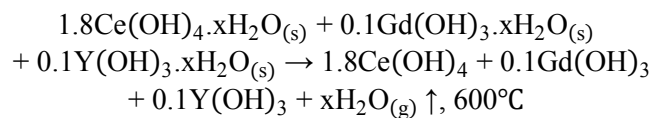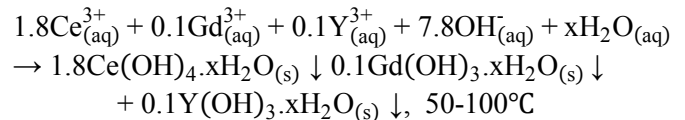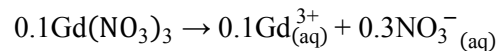
Materials and Experimantal Procedures

Preparation of $Ce_{0.9}Gd_{0.1}O_{2-\delta}$–$Ce_{0.9}Y_{0.1}O_{2-\delta}$ nano ceramic composite material with and without addition of surfactant by chemical precipitation method

The chemicals such as, $Ce(NO_3)_3.6H_2O$ (99.0%, Himedia, India), Gd_2O_3 (99.9%, Loba Chemie, India), Y_2O_3 (99.9%, Loba Chemie, India), sodium hydroxide (≥97%, Merck, India) and poly(vinyl alcohol) (99%, Merck, India) were used in the preparation of $Ce_{0.9}Gd_{0.1}O_{2-\delta}$-$Ce_{0.9}Y_{0.1}O_{2-\delta}$ nanoceramic composite material. Initially, reagents such as, 0.025 M of $Gd(NO_3)_3$ (0.45 g of Gd_2O_3 is dissolved in 10 ml HNO_3 and made up to 100 ml with distilled water), 0.025 M of $Y(NO_3)_3$ (0.2822 g of Y_2O_3 is dissolved in 10 ml HNO_3 and made up to 100 ml with distilled water), 0.45M of $Ce(NO_3)_3.6H_2O$ (19.53 g of $Ce(NO_3)_3$ in 100 ml of distilled water) and 1.95 M of NaOH (7.8 g of sodium hydroxide in 100 ml of distilled water) were prepared. Sodium hydroxide solution was taken in a 500 ml beaker To this sodium hydroxide solution, nitrate salt solutions such as, $Ce(NO_3)_3$, $Gd(NO_3)_3$ and $Y(NO_3)_3$ solutions were added slowly one by one with the help of a burette and the entire mixture was stirred perfectly in a magnetic stirring apparatus at a speed of 1,000 rpm at room temperature for an hour. Throughout the experiment, the pH was adjusted to pH > 9 with the addition of alkali as reported [23]. The resultant yellow coloured precipitate [$Ce(OH)_4$+$Gd(OH)_3$+$Y(OH)_3$] was filtered, and then washed with deionized water and ethanol (9:1 volume ratio) for 2 to 3 times and dried at 50-100°C for 3 h. The dried precipitate was heat treated at 300°C, 450°C, 600°C and 750°C for 2 h each. During the calcination process, phase pure yellow coloured $Ce_{0.9}Gd_{0.1}O_{2-\delta}$-$Ce_{0.9}Y_{0.1}O_{2-\delta}$ nanoceramic composite material was formed. To study the particle characteristics of the final product, the same experiment was repeated with the addition of

surfactant (2 ml of 10% PVA) in the initial stage along with the precipitant (sodium hydroxide) and the remaining steps were carried out as described earlier. Main reactions occur during the experimental procedure can be written briefly as follows:

Reaction mechanism involved in the preparation of $Ce_{0.9}Gd_{0.1}O_{2-\delta}$–$Ce_{0.9}Y_{0.1}O_{2-\delta}$
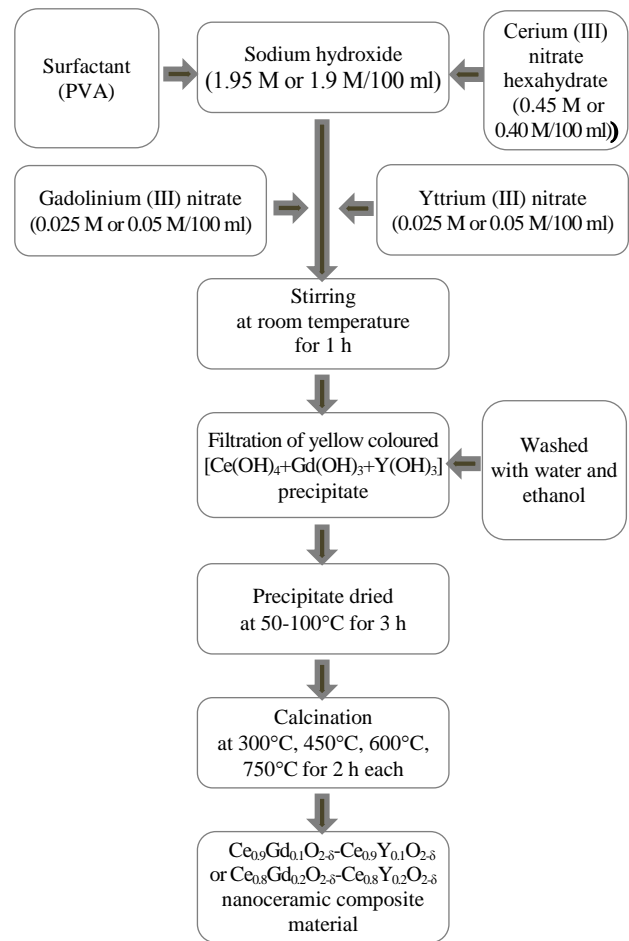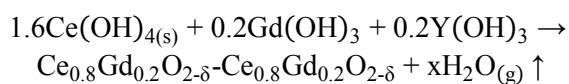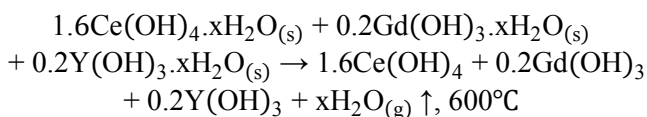
$$7.8NaOH \rightarrow 7.8Na^+_{(aq)} + 7.8OH^-_{(aq)}$$

$$1.8Ce(NO_3)_3.6H_2O_{(s)} \rightarrow$$
$$1.8Ce^{3+}_{(aq)} + 5.4NO_3^-{}_{(aq)} + 6H_2O_{(aq)}$$

$$0.1Gd(NO_3)_3 \rightarrow 0.1Gd^{3+}_{(aq)} + 0.3NO_3^-{}_{(aq)}$$

$$0.1Y(NO_3)_3 \rightarrow 0.1Y^{3+}_{(aq)} + 0.3NO_3^-{}_{(aq)}$$

$$1.8Ce^{3+}_{(aq)} + 0.1Gd^{3+}_{(aq)} + 0.1Y^{3+}_{(aq)} + 7.8OH^-_{(aq)} + xH_2O_{(aq)}$$
$$\rightarrow 1.8Ce(OH)_4.xH_2O_{(s)} \downarrow 0.1Gd(OH)_3.xH_2O_{(s)} \downarrow$$
$$+ 0.1Y(OH)_3.xH_2O_{(s)} \downarrow, \ 50\text{-}100°C$$

$$1.8Ce(OH)_4.xH_2O_{(s)} + 0.1Gd(OH)_3.xH_2O_{(s)}$$
$$+ 0.1Y(OH)_3.xH_2O_{(s)} \rightarrow 1.8Ce(OH)_4 + 0.1Gd(OH)_3$$
$$+ 0.1Y(OH)_3 + xH_2O_{(g)} \uparrow, \ 600°C$$

$$1.8Ce(OH)_{4(s)} + 0.1Gd(OH)_3 + 0.1Y(OH)_3 \rightarrow$$
$$Ce_{0.9}Gd_{0.1}O_{2-\delta}\text{-}Ce_{0.9}Gd_{0.1}O_{2-\delta} + xH_2O_{(g)} \uparrow$$

Preparation of $Ce_{0.8}Gd_{0.2}O_{2-\delta}$–$Ce_{0.8}Y_{0.2}O_{2-\delta}$ nano ceramic composite material with and without addition of surfactant by chemical precipitation method

The chemicals such as, $Ce(NO_3)_3.6H_2O$ (99.0%, Himedia, India), Gd_2O_3 (99.9%, Loba Chemie, India), Y_2O_3(99.9%, Loba Chemie, India), sodium hydroxide (≥97%, Merck, India) and poly(vinyl alcohol) (99%, Merck, India) were used in the preparation of $Ce_{0.9}Gd_{0.1}O_{2-\delta}$-$Ce_{0.9}Y_{0.1}O_{2-\delta}$ nanoceramic composite material. Initially, reagents such as, 0.05 M of $Gd(NO_3)_3$ (0.90 g of Gd_2O_3 is dissolved in 10 ml HNO_3 and made up to 100 ml with distilled water), 0.05M of $Y(NO_3)_3$ (0.564 g of Y_2O_3 is dissolved in 10 ml HNO_3 and made up to 100 ml with distilled water), 0.40 M of $Ce(NO_3)_3.6H_2O$ (17.28 g of $Ce(NO_3)_3$ in 100 ml of distilled water) and 1.90 M of NaOH (7.6 g of sodium hydroxide in 100 ml of distilled water) were prepared. Sodium hydroxide solution was taken in a 500 ml beaker. To this sodium hydroxide solution, nitrate salt solutions such as, $Ce(NO_3)_3$, $Gd(NO_3)_3$

and $Y(NO_3)_3$ solutions were added slowly one by one with the help of a burette and the entire mixture was stirred perfectly in a magnetic stirring apparatus at a speed of 1,000 rpm at room temperature for an hour. Throughout the experiment, the pH was adjusted to pH > 9 with the addition of alkali. The resultant yellow coloured precipitate [$Ce(OH)_4$+ $Gd(OH)_3$ + $Y(OH)_3$] was filtered and then washed with deionized water and ethanol (9:1 ratio) for 2 to 3 times and dried at 50-100°C for 3 h. The dried precipitate was heat treated at 300°C, 450°C, 600°C and 750°C for 2 h each. During the calcination process, phase pure yellow coloured $Ce_{0.8}Gd_{0.2}O_{2-\delta}$– $Ce_{0.8}Y_{0.2}O_{2-\delta}$ nanoceramic composite material was formed. To study the particle characteristics of the final product, the same experiment was repeated with the addition of surfactant (2 ml of 10% PVA) in the initial stage along with the precipitant (sodium hydroxide) and the remaining steps were carried out as indicated earlier. Figure 1 shows a schematic illustration of the synthesis of nanocomposite materials by chemical precipitation process. Main reactions occur during the experimental procedure can be written briefly as follows:

Reaction mechanism involved in the preparation of $Ce_{0.8}Gd_{0.2}O_{2-\delta}$–$Ce_{0.8}Y_{0.2}O_{2-\delta}$

$$7.6NaOH \rightarrow 7.6Na^+_{(aq)} + 7.6OH^-_{(aq)}$$

$$1.6Ce(NO_3)_3.6H_2O_{(s)} \rightarrow$$
$$1.6Ce^{3+}_{(aq)} + 4.8NO_3^-{}_{(aq)} + 6H_2O_{(aq)}$$

$$0.2Gd(NO_3)_3 \rightarrow 0.2Gd^{3+}_{(aq)} + 0.6NO_3^-{}_{(aq)}$$

$$0.2Y(NO_3)_3 \rightarrow 0.2Y^{3+}_{(aq)} + 0.6NO_3^-{}_{(aq)}$$

$$1.6Ce^{3+}_{(aq)} + 0.2Gd^{3+}_{(aq)} + 0.2Y^{3+}_{(aq)} + 7.6OH^-_{(aq)} + xH_2O_{(aq)}$$
$$\rightarrow 1.6Ce(OH)_4.xH_2O_{(s)} \downarrow + 0.2Gd(OH)_3.xH_2O_{(s)} \downarrow$$
$$+ 0.2Y(OH)_3.xH_2O_{(s)} \downarrow, \ 50\text{-}100℃$$

$$1.6Ce(OH)_4.xH_2O_{(s)} + 0.2Gd(OH)_3.xH_2O_{(s)}$$
$$+ 0.2Y(OH)_3.xH_2O_{(s)} \rightarrow 1.6Ce(OH)_4 + 0.2Gd(OH)_3$$
$$+ 0.2Y(OH)_3 + xH_2O_{(g)} \uparrow, \ 600℃$$

$$1.6Ce(OH)_{4(s)} + 0.2Gd(OH)_3 + 0.2Y(OH)_3 \rightarrow$$
$$Ce_{0.8}Gd_{0.2}O_{2-\delta}\text{-}Ce_{0.8}Gd_{0.2}O_{2-\delta} + xH_2O_{(g)} \uparrow$$
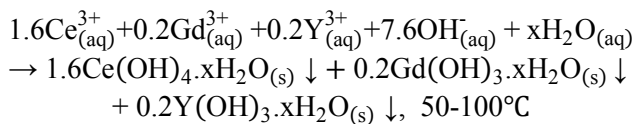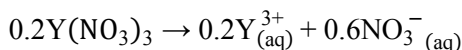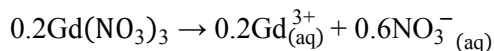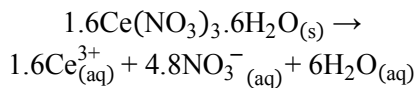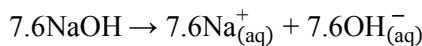
Figure 1. Schematic illustration of the synthesis of $Ce_{0.9}Gd_{0.1}O_{2-\delta}$-$Ce_{0.9}Y_{0.1}O_{2-\delta}$ and $Ce_{0.8}Gd_{0.2}O_{2-\delta}$-$Ce_{0.8}Y_{0.2}O_{2-\delta}$ nanoceramic composite materials by chemical precipitation process.

Characterization of the nanoceramic composite materials

The prepared powers were subjected to characterization after calcination at 750°C for 2 h. The powder X-ray diffraction (XRD) studies were carried out using Shimadzu XRD 6000 X-ray diffractometer at a scan speed of 5 deg/min using CuKα radiation at room temperature. The lattice parameters were calculated by least square fitting method using DOS computer programming. The theoretical density of the powders was calculated with the obtained XRD data. The crystallite sizes of the powder were calculated by Scherrer's formula. Bruker IFS 66V FT-IR spectrometer was employed to record the FT-IR spectra of nanoceramic composite materials in the range of 4,000-400 cm^{-1}. The particle size of the powder was measured using Malvern Particle Size Analyzer using triple distilled water as medium. The surface morphology of the particles was studied by means of JEOL Model JSM-6360 scanning electron microscope.

Results and Discussion

XRD studies

The XRD patterns of the ceria based nanoceramic composite oxide materials prepared by the chemical precipitation method with and without the addition of surfactant (PVA) are shown in Figures 2(a)-2(b) and 3(a)-3(b) respectively. It is reported that co-doped ceria $Ce_{1-x}Gd_{x-y}Y_yO_{2-0.5x}$ (x=0.15 and 0.2, $0 \leq y \leq x$) prepared by glycine-nitrate method indexed as fluorite geometry [7]. It is reported that the crystal structure of $Ce_{0.9}Gd_{0.1}O_{1.95}$ prepared by sol-gel method is found to be cubic [21, 24]. Xu, L.H. et al., (2007) have reported fluorite structure for $Ce_{0.9}Sm_{0.1}O_{1.95}$ prepared by RF magnetron sputtering growth [25]. In our case, the XRD patterns of the heat treated powders reveal the formation of well-crystallined single phase materials with cubic fluorite structure. No extra peaks corresponding to any other secondary phases are observed. The XRD patterns obtained of the ceria based nanoceramic composite oxide materials were compared with the standard data for CeO_2 (JCPDS card No. 34-0394). The lattice parameters are calculated from 2θ values in the X-ray diffraction patterns by using DOS computer programming. The theoretical density (D_X) for the samples was calculated according to the formula [26].

$$D_x = \frac{Z \times M}{N \times a^3} \qquad (1)$$

Where, Z = number of chemical species in the unit cell, M = molecular mass of the sample (g/mol), N = Avogadro's number (6.022×10^{23}) and a = lattice constant, cm. Crystallite size of the samples was calculated from XRD line broadening method using the following Scherrer relationship [27]:

$$D_p = \frac{k\lambda}{\beta \cos \theta} \qquad (2)$$

Where 'D_p' is the crystallite size, 'k' is a numerical constant (~0.9), 'λ' is the wavelength of X-rays (for CuKα radiation, λ = 1.5418 Å), 'β' is the effective broadening taken as a full width at half maximum (FWHM) (in radians), 'θ' is the diffraction angle for the peak. The crystallographic parameters obtained on the ceria based nanoceramic composite materials are given in Table 1. The crystallite size of samaria doped ceria particles obtained by spray pyrolysis

was reported to be 9.5-14.2 nm [28]. The theoretical density of ceria powder synthesized by glycine-nitrate synthesis was found to be 7.13 g/cc [29]. However, our crystallite size values were found in the range of 7.12-10.22 nm. The theoretical density values are found to be in the range of 7.00 g/cc which is similar to the reported data [29]. Other crystalline parameters are in line with the reported data for doped ceria materials. Also, from Table 1, it is found that the powders prepared with PVA as surfactant have less crystalline size values. It is reported that the addition of surfactants in the precursor solutions leads to reduction in crystallite size of particle significantly [30]. From this, it is understood that PVA (surfactant) plays key role in the final size of the particles
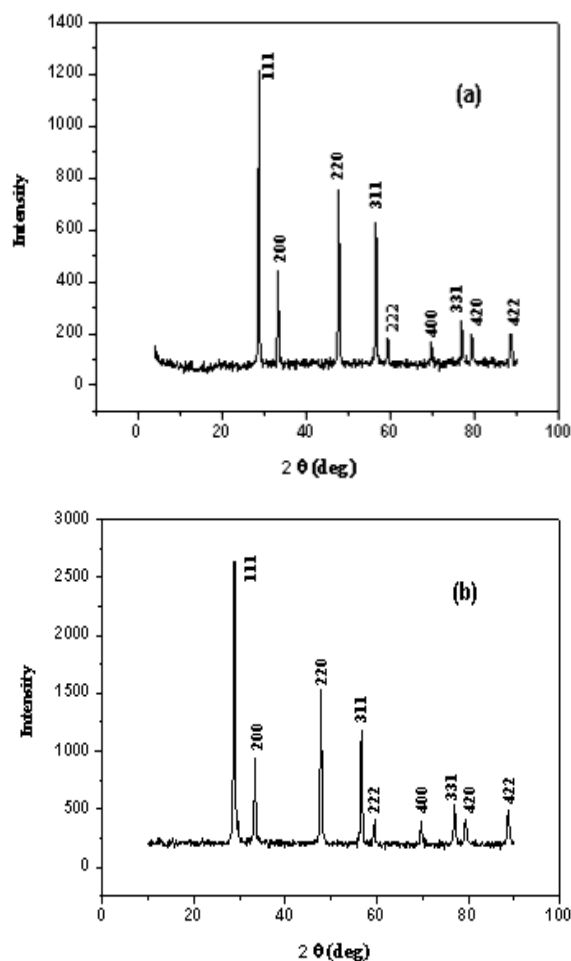
Figure 2. XRD patterns obtained on (a) $Ce_{0.9}Gd_{0.1}O_{2-\delta}$-$Ce_{0.9}Y_{0.1}O_{2-\delta}$ (without surfactant) and (b) $Ce_{0.9}Gd_{0.1}O_{2-\delta}$-$Ce_{0.9}Y_{0.1}O_{2-\delta}$ (with surfactant, PVA) prepared by chemical precipitation method

Table 1 Crystallographic parameters obtained on the ceria based nano ceramic-based composite materials.

Sample	Crystal structure	Unit cell parameter 'a' (Å)	Unit cell volume (Å^3)	Crystallite size (nm)	Theoretical density (g/cc)
CeO_2 (JCPDS No. 34-0394)	Cubic (FC)	5.4113	158.4581	--	7.2200
$Ce_{0.9}Gd_{0.1}O_{2-\delta}$-$Ce_{0.9}Y_{0.1}O_{2-\delta}$	Cubic (FC)	5.4140	158.6918	10.22	7.0983
$Ce_{0.9}Gd_{0.1}O_{2-\delta}$-$Ce_{0.9}Y_{0.1}O_{2-\delta}$ with PVA	Cubic (FC)	5.4446	161.3979	8.58	6.9793
$Ce_{0.8}Gd_{0.2}O_{2-\delta}$-$Ce_{0.8}Y_{0.2}O_{2-\delta}$	Cubic (FC)	5.4096	158.3053	9.28	7.0777
$Ce_{0.8}Gd_{0.2}O_{2-\delta}$-$Ce_{0.8}Y_{0.2}O_{2-\delta}$ with PVA	Cubic (FC)	5.4548	162.2174	7.12	6.9070
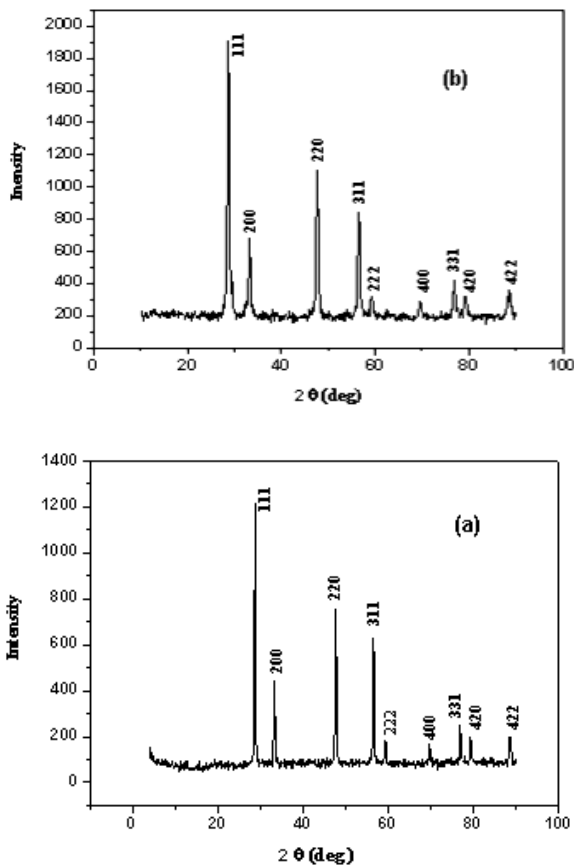
Figure 3. XRD patterns obtained on (a) $Ce_{0.8}Gd_{0.2}O_{2-\delta}$-$Ce_{0.8}Y_{0.2}O_{2-\delta}$ (without surfactant) and (b) $Ce_{0.8}Gd_{0.2}O_{2-\delta}$-$Ce_{0.8}Y_{0.2}O_{2-\delta}$ (with surfactant, PVA) prepared by chemical precipitation method.

FT-IR Studies

Figures 4(a)-4(c) show the FT-IR spectrums obtained on nanoceramic composite materials prepared by the chemical precipitation method. FT-IR measurements were done using KBr method at room temperature (RT). In all the FTIR spectrums, presence of band at wave number below 500 cm^{-1} corresponds to the Ce-O band as reported [31]. The intensive band at 1,383 cm^{-1} represents N-O stretch due to the presence of traces of nitrate in the samples as indicated in the literature [32]. The samples showed peaks at around 2,300 cm^{-1}, are due to the presence of dissolved or atmospheric CO_2 in the sample [33]. The peak appeared at 1,600 cm^{-1} is attributable to H-O-H bending mode and is indicative of the presence of molecular water in the samples [31]. Most of the peaks observed in FT-IR spectra are similar to each powder which shows the structural similarity in all the samples.

Particle size Measurements

The prepared nanoceramic composite materials were subjected to particle size measurements using Malvern particle size analyzer with triple distilled water as medium. Prior to particle size measurements, the samples were sonicated in triple distilled water for about 5 min. The particle size distribution curves of nanoceramic composite materials are shown in Figures 5(a)-5(d).

Particle size distribution data of $Ce_{0.9}Gd_{0.1}O_{2-\delta}$-$Ce_{0.9}Y_{0.1}O_{2-\delta}$ powder prepared by chemical precipitation method without and with surfactant (PVA)

The particle size distribution curves obtained with $Ce_{0.9}Gd_{0.1}O_{2-\delta}$-$Ce_{0.9}Y_{0.1}O_{2-\delta}$ powder prepared by chemical precipitation method without and with surfactant (PVA) are shown in Figure 5(a)-5(c). The particle characteristics obtained on $Ce_{0.9}Gd_{0.1}O_{2-\delta}$-$Ce_{0.9}Y_{0.1}O_{2-\delta}$ powders are indicated in Table 2.

From Figure 5(a)-5(c) and the particle characteristics data (Table 2), it was understood that the average particle size of powder prepared by the chemical precipitation method is found to be 218.6 nm (without surfactant) and 146.7 nm (with PVA).
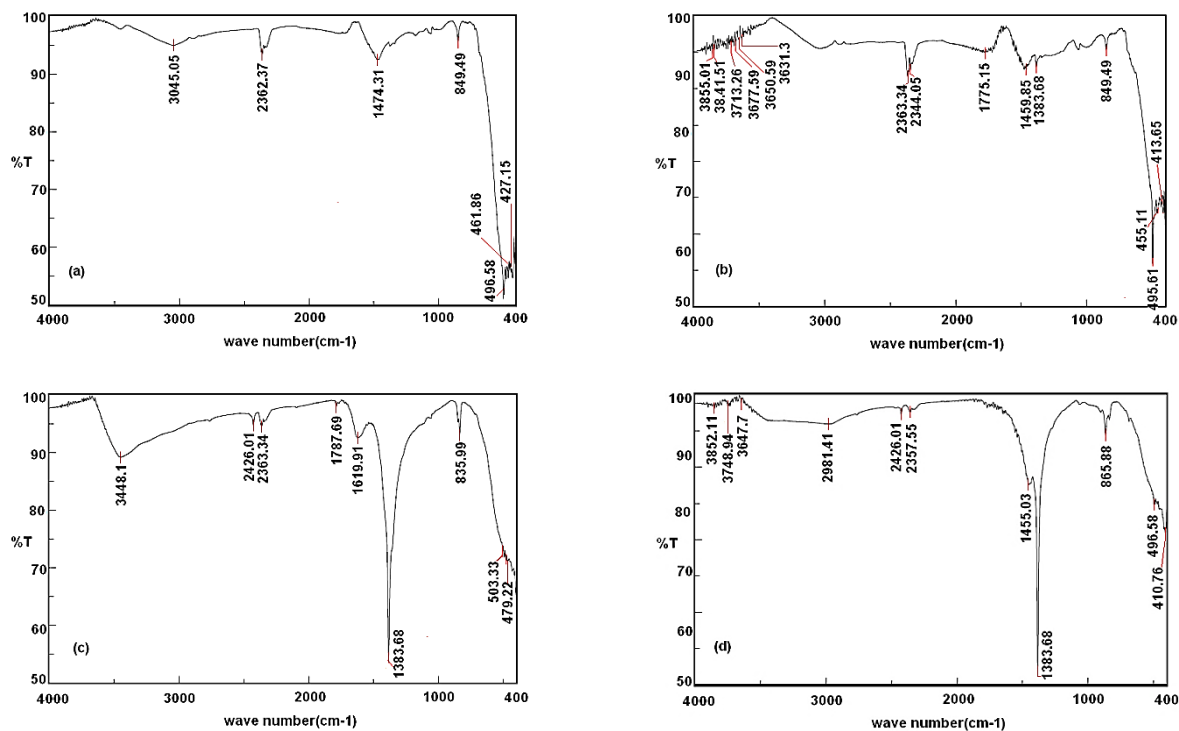
Figure 4. FT-IR spectrums obtained on (a) $Ce_{0.9}Gd_{0.1}O_{2-\delta}$- $Ce_{0.9}Y_{0.1}O_{2-\delta}$ (without surfactant); (b) $Ce_{0.8}Gd_{0.2}O_{2-\delta}$-$Ce_{0.8}Y_{0.2}O_{2-\delta}$ (without surfactant); (c) $Ce_{0.9}Gd_{0.1}O_{2-\delta}$-$Ce_{0.9}Y_{0.1}O_{2-\delta}$ (with surfactant, PVA) and (d) $Ce_{0.8}Gd_{0.2}O_{2-\delta}$-$Ce_{0.8}Y_{0.2}O_{2-\delta}$ (with surfactant, PVA) prepared by chemical precipitation method.
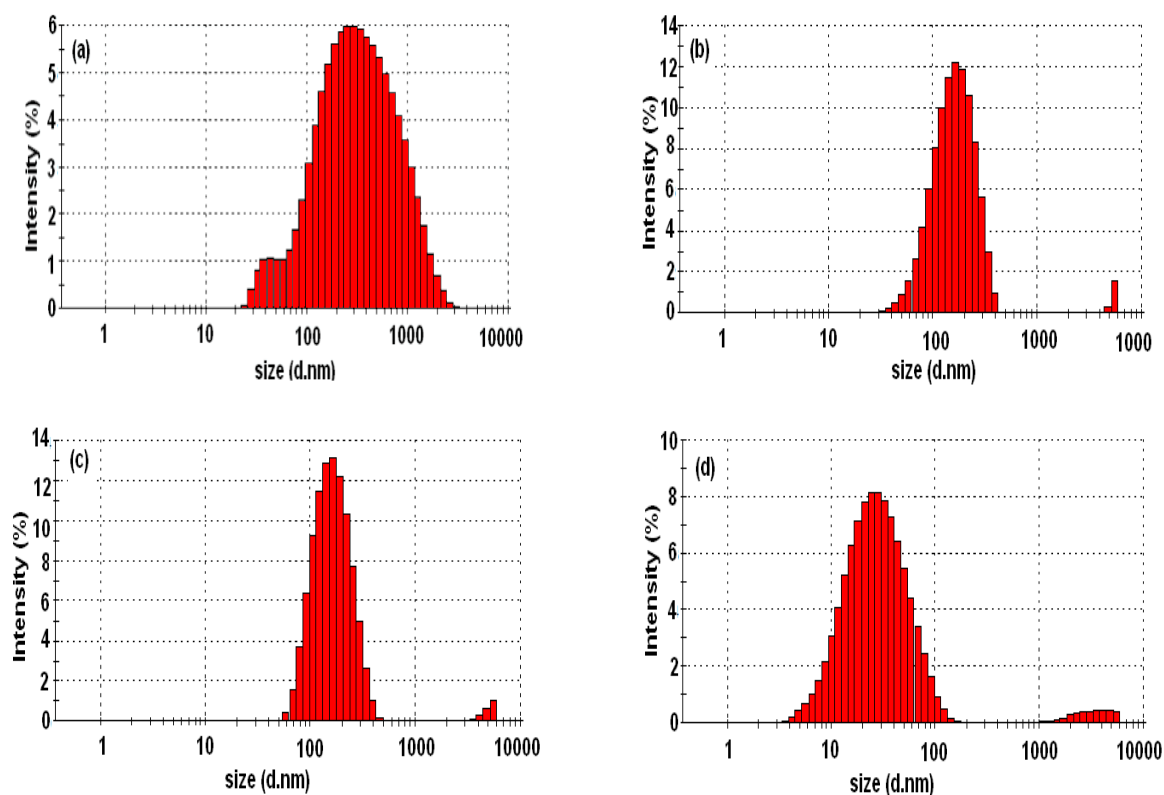
Figure 5. Particle size curves obtained on (a) $Ce_{0.9}Gd_{0.1}O_{2-\delta}$- $Ce_{0.9}Y_{0.1}O_{2-\delta}$ (without surfactant) -218.6 nm; (b) $Ce_{0.8}Gd_{0.2}O_{2-\delta}$-$Ce_{0.8}Y_{0.2}O_{2-\delta}$ (without surfactant) -165.5 nm; (c) $Ce_{0.9}Gd_{0.1}O_{2-\delta}$- $Ce_{0.9}Y_{0.1}O_{2-\delta}$ (with surfactant, PVA)-146.7 nm and (d) $Ce_{0.8}Gd_{0.2}O_{2-\delta}$-$Ce_{0.8}Y_{0.2}O_{2-\delta}$ (with surfactant, PVA) prepared by chemical precipitation method -22.88 nm.

Table 2. Particle characteristics data obtained on $Ce_{0.9}Gd_{0.1}O_{2-\delta}$-$Ce_{0.9}Y_{0.1}O_{2-\delta}$ powder prepared by chemical precipitation method without and with surfactant (PVA).

Sample	Peak 1		Peak 2		Average particle size (nm)
	Intensity (%)	Diameter (nm)	Intensity (%)	Diameter (nm)	
$Ce_{0.9}Gd_{0.1}O_{2-\delta}$-$Ce_{0.9}Y_{0.1}O_{2-\delta}$ (without surfactant)	95.6	463.7	4.4	40.36	218.6
$Ce_{0.9}Gd_{0.1}O_{2-\delta}$-$Ce_{0.9}Y_{0.1}O_{2-\delta}$ (without surfactant-PVA)	98.0	171.6	2.0	50.57	146.7

Table 3. Particle characteristics data obtained on $Ce_{0.8}Gd_{0.2}O_{2-\delta}$-$Ce_{0.8}Y_{0.2}O_{2-\delta}$ powder prepared by chemical precipitation method without and with surfactant (PVA).

Sample	Peak 1		Peak 2		Average particle size (nm)
	Intensity (%)	Diameter (nm)	Intensity (%)	Diameter (nm)	
$Ce_{0.8}Gd_{0.2}O_{2-\delta}$-$Ce_{0.8}Y_{0.2}O_{2-\delta}$ (without surfactant)	98.1	170.0	1.9	54.31	165.5
$Ce_{0.8}Gd_{0.2}O_{2-\delta}$-$Ce_{0.8}Y_{0.2}O_{2-\delta}$ (without surfactant-PVA)	96.5	32.39	3.5	33.63	22.88

Particle size distribution data of $Ce_{0.8}Gd_{0.2}O_{2-\delta}$– $Ce_{0.8}Y_{0.2}O_{2-\delta}$ powder prepared by chemical precipitation method without and with surfactant (PVA)

The particle size distribution curves obtained with $Ce_{0.8}Gd_{0.2}O_{2-\delta}$-$Ce_{0.8}Y_{0.2}O_{2-\delta}$ powder prepared by chemical precipitation method without and with surfactant (PVA) are shown in Figure 5 b-d. The particle characteristics obtained on $Ce_{0.8}Gd_{0.2}O_{2-\delta}$–$Ce_{0.8}Y_{0.2}O_{2-\delta}$ powder are indicated in Table 3.

From Figure 5(b)-5(d) and the particle characteristics data (Table 3), it was understood that the average particle size of powder prepared by the chemical precipitation method is found to be 165.5 nm (without surfactant) and 22.88 nm (with PVA). The larger particles present in the powder may be due to high temperature treatment.

From the results, it was clearly understood that the addition of surfactant consistently reduced the particle size of the final powder as reported in the literature[34]

Scanning Electron Microscopic (SEM) studies

SEM pictures obtained on $Ce_{0.9}Gd_{0.1}O_{2-\delta}$–$Ce_{0.9}Y_{0.1}O_{2-\delta}$ powder prepared by chemical precipitation method without and with surfactant (PVA)

SEM analysis provides the information about the size and shape of the particle and pore. The SEM photographs obtained on $Ce_{0.9}Gd_{0.1}O_{2-\delta}$-$Ce_{0.9}Y_{0.1}O_{2-\delta}$ (without PVA) and $Ce_{0.9}Gd_{0.1}O_{2-\delta}$-$Ce_{0.9}Y_{0.1}O_{2-\delta}$ (with surfactant, PVA) are indicated in Figures 6(a)-6(b) and 7(a)-7(b) respectively. From the photographs, it was understood that fine particles between the range of 50-150 nm were present in the samples. Also, it was found that addition of surfactant has made significant changes in the final particle size of the powder.

SEM analysis provides the information about the size and shape of the particle and pore. The SEM pictures obtained on $Ce_{0.8}Gd_{0.2}O_{2-\delta}$-$Ce_{0.8}Y_{0.2}O_{2-\delta}$ (without PVA) and $Ce_{0.8}Gd_{0.2}O_{2-\delta}$-$Ce_{0.8}Y_{0.2}O_{2-\delta}$ (with surfactant, PVA) are shown in Figures 8(a)-8(b) and 9(a)-9(b) respectively. From the SEM studies, it was found that the grain size of the powders were found in the range of 40-200 nm. In this case also, the addition of surfactant has affected the final particle characteristics of the powder. From the SEM studies, it was understood that the addition of surfactants influenced the final particle as described by particle characteristics dat
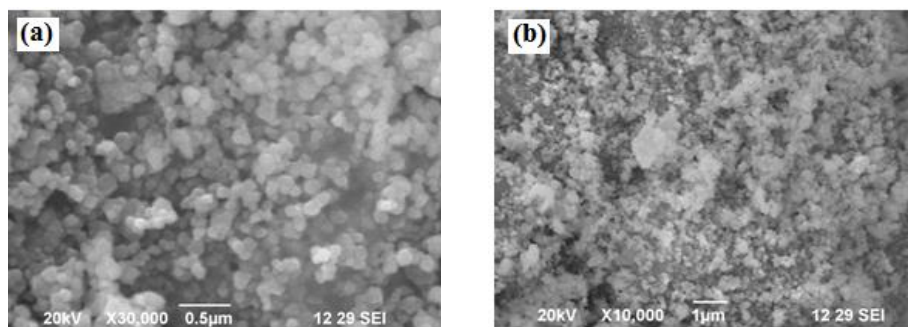
RAKHIKA, D. and NESARAJ, A.S.
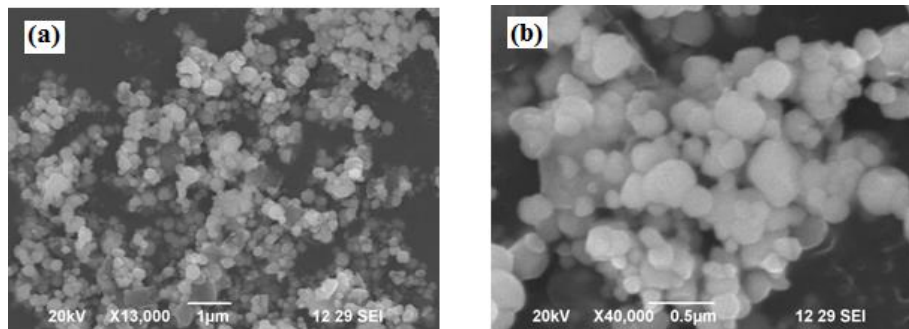
Figure 6. SEM photographs obtained on $Ce_{0.9}Gd_{0.1}O_{2-\delta}$-$Ce_{0.9}Y_{0.1}O_{2-\delta}$ (without surfactant) prepared by chemical precipitation method.
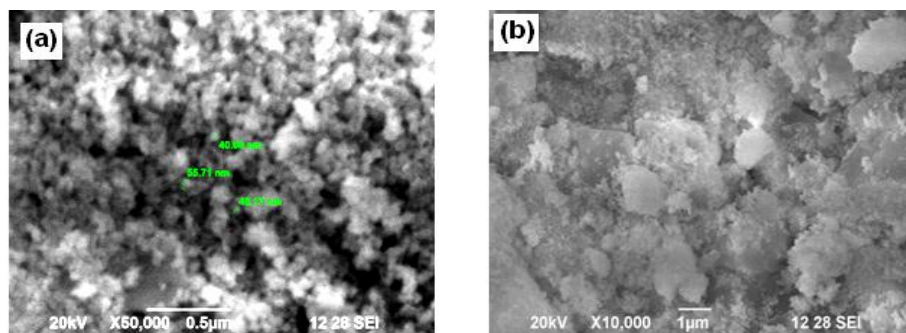
Figure 7. SEM photographs obtained on $Ce_{0.9}Gd_{0.1}O_{2-\delta}$- $Ce_{0.9}Y_{0.1}O_{2-\delta}$ (with surfactant, PVA) prepared by chemical precipitation method.

Figure 8. SEM photographs obtained on $Ce_{0.8}Gd_{0.2}O_{2-\delta}$-$Ce_{0.8}Y_{0.2}O_{2-\delta}$ (without surfactant) prepared by chemical precipitation method.
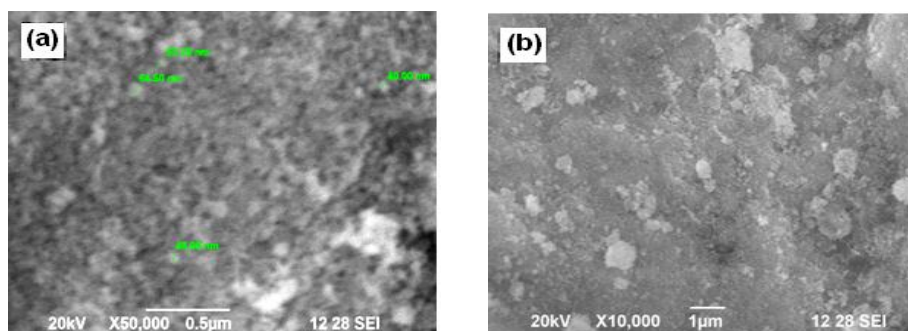
Figure 9. SEM photograph obtained on $Ce_{0.8}Gd_{0.2}O_{2-\delta}$ -$Ce_{0.8}Y_{0.2}O_{2-\delta}$ (with surfactant, PVA) prepared by chemical precipitation method.

Conclusions

Chemical precipitation process can be effectively used for the preparation of ceria based nanoceramic composite materials. The powder XRD data obtained on nano-ceramic composite powders of $Ce_{0.9}Gd_{0.1}O_{2-\delta}$–$Ce_{0.9}Y_{0.1}O_{2-\delta}$ and $Ce_{0.8}Gd_{0.2}O_{2-\delta}$-$Ce_{0.8}Y_{0.2}O_{2-\delta}$ is in agreement with the standard reported JCPDS data. From the FTIR spectra of nano composite powders, it is observed that characteristic peak of CeO_2 is present in all four samples. The particle size analysis data obtained on powders suggest that the particles are present in nano diameter range. However, presence of few micron sized particles may be due to high temperature treatment. From the SEM studies, it was found that the presence of surfactant has influenced the particle characteristics of the powder.

Acknowledgments

References

1. Rampon, R., Toma, F.L., Bertrand, G. and Coddet, C. (2006). Liquid plasma sprayed coatings of yttria-stabilized zirconia for SOFC electrolytes. *J. Thermal Spray Tech.,* **15(4)**: 682-688.

2. Aneggi, E., Liorca, J., Boaro, M. and Trovarelli, A. (2005). Surface-structure sensitivity of CO oxidation over polycrystalline ceria powders. *J. Catal*., **234**: 88-95.

3. Deng, W. and Flytzani-Stephanopoulos, M. (2006). On the deactivation of nano-structured gold-ceria and platinum-ceria catalysts for the water-gas shift reaction in practical fuel cell applications. *Angew. Chem. Int. Ed.*, **45**: 2285-2289.

4. Wang, S., Kobayashi, T., Dokiya, M. and Hashimoto, T. (2000). Electrical and ionic conductivity of Gd-doped ceria. *J. Electrochem. Soc.*, **147(10)**: 3606-3609.

5. Hari Prasad, D., Kim, H.R., Park, J.S., Son, J.W., Kim, B.K., Lee, H.W. and Lee, J.H. (2012). Cobalt oxide co-doping effect on the sinterability and electrical conductivity of nano-crystalline Gd - doped ceria. *Ceram. Int*., **38**: 497-500.

6. Zhen, Y.D., Tok, A.I.Y., Jiang, S.P. and Boey, F.Y.C. (2008). Fabricatio and performance of gadolinia-doped ceria-based intermediate-temperature solid oxide fuel cells. *J. Power Sources*., **178(1)**: 69-74.

7. Zheng, Y., Shi, Y., Gu, H., Gao, L., Chen, H. and Guo, L. (2009). La and Ca co-doped ceria-based electrolyte materials for IT-SOFCs. *Mater. Res. Bull*., **43(4)**: 1046-1054.

8. Samson Nesaraj, A., Arul Raj, I.and Pattabiraman, R. (2007). Synthesis and characterization of $LaCoO_3$ based cathode and its chemical compatibility with CeO_2 based electrolyte in intermediate temperature solid oxide fuel cells (ITSOFC). *Indian J. Chem. Technol*., **14**: 154-160.

9. Van herle, J., Horia, T., Kawada, T., Sakai, N., Yokokawa, H. and Dokia, M. (1996). Low temperature fabrication of (Y,Gd,Sm)-doped ceria electrolyte. *Solid State Ionics.*, **86(8)**: 1255-1258.

10. Zhen, Y.D., Tok, A.I.Y., Jiang, S.P. and Boey, F.Y.C. (2008). Fabrication & Performance of GDC-based intermediate-temperature Solid Oxide Fuel Cells., *J. Power Sources*., **178**: 69-74.

11. Lapa, C. M., Figueiredo, F. M. L., de Souza, D.P.F., Song, L., Zhu, B. and Marques, F. M. P. (2010). Synthesis and characteri-zation of composite electrolytes based on samaria-doped ceria and Na/Li carbonates. *Int. J. Hydrogen Energy*., **35**: 2953-2957.

12. Zha, S., Xia, C. and Meng, G. (2003). Effect of Gd (Sm) doping on properties of ceria electrolyte for solid oxide fuel cells. *J. Power Sources*., **115(1)**: 44-48.

13. Hirano, M., Watanabe, S., Kato, E., Mizutani, Y., Kawai, M. and Nakamura, Y. (1999). High electrical conductivity and high fracture strength of Sc_2O_3-doped zirconia ceramics with submicrometre grains. *J. Am. Ceram. Soc*., **82(10)**: 2861-2864.

14. Kirk, N.B. and Wood, J. V. (1995). The effect of the calcinations process on the crystallite shape of sol-gel cerium oxide used for glass polishing. *J. Mater. Sci*., **30(8)**: 2171-2175.

15 Xia, B., Lenggoro, I.W. and Okuyama, K. (2001). Synthesis of CeO2 nanoparticles by salt-assisted ultrasonic aerosol decomposition. *J. Mater. Chem*., **11(12)**: 2925-2927.

16. Lenka, R.K., Mahata, T., Sinha, P.K. and Tyagi, A.K. (2008). Combustion synthesis of gadolinia-doped ceria using glycine and urea fuels. *J. Alloys Compd.,* **466**: 326-329.

17. Sha, X.Q., Lu, Z., Huang, X.Q., Miao, J.P., Ding, Z.H., Xin, X.S. and Su, W.H. (2007). Study on La and Y co-doped ceria-based electrolyte materials. *J. Alloys Compd*., **428(1-2)**: 59-64.

18. Yifeng, Z., Liqiang, W., Haitao, G., Ling, G.,Han, C. and Lucun, G. (2009). The effect of Sr on the properties of Y-doped ceria electrolyte for IT-SOFCs. *J. Alloys Compd*., **486(1-2)**:586-589.

19. Prasad, D.H., Son, J.W., Kim, B.K. and Lee, H.W. (2008). Synthesis of nano-crystalline $Ce_{0.9}Gd_{0.1}O_{1.95}$ electrolyte by novel sol-gel thermolysis process for IT-SOFCs. *J. Eur. Ceram. Soc*., **28**: 3107-3112.

20. Kayalvizhi, M. and John Berchmans, L. (2010). Combustion synthesis of Lanthanum substituted $LiNiO_2$ using Hexamine as a fuel. *E-J.Chem*., **7(S1)**: S137-S142.

21. Tao, Y., Shao, J., Wang, J. and Wang, G. (2009). Morphology control of $Ce_{0.9}Gd_{0.1}O_{1.95}$ nano powder synthesized by sol-gel method using PVP as a surfactant. *J. Alloys Compd*., **484**: 729-733.

22. Ding, C., Lin, H., Sato, K. and Hashida, T. (2009). Synthesis of $NiO-Ce_{0.9}Gd_{0.1}O_{1.95}$ nanocomposite powders for low temperature solid oxide fuel cell anodes by co-precipitation. *Scr. Mater*., **60(4)**: 254-256.

23. Choy, J.H., Han, Y.S. and Kim, J.T. (1995). Hydroxide coprecipitation route to the piezoelectric oxide Pb(Zr,Ti)O3(PZT). *J. Mater. Chem. A.,* **5**: 65-69.

24. Fuentes, R.O. and Baker, R.T. (2008). Synthesis and properties of Gadolinium-doped ceria solid solutions for IT-SOFC electrolytes. *Int. J. Hydrogen Energy*., **33(13)**: 3480-3484.

25. Xu, L.H., Xu, Y.X., Wang, C. and Wang, T.M. (2007). Preparation and Properties of $Ce_{0.9}Sm_{0.1}O_{1.95}$ as the Electrolytes of IT-SOFC. *Key Eng. Mater*., **336-338**: 398-400.

26. Fu, Y.P. (2009). Electrical conductivity and magnetic properties of $Li_{0.5}Fe_{2.5-x}Cr_xO_4$ ferrite. *Mater. Chem. Phys*., **115(1)**: 334-338.

27. Verma, S., Pradhan, S.D., Pasricha, R., Sainkar, S.R. and Joy, P.A. (2005). A novel low temperature synthesis of nano- sized NiZn ferrite. *J.Am. Ceram. Soc.*, **88(9)**:2597-2599.

28. Pichestapong, P. and Injarean, U. (2010). Preparation of Samaria-Doped Ceria Nanoparticles by Spray Pyrolysis. *J. Met. Mater. Miner*., **20(2)**: 51-54.

29. Purohit, R.D., Sharma, B.P., Pillai, K.T. and Tyagi, A.K. (2001). Ultrafine ceria powders via glycine-nitrate combustion. *Mater. Res. Bull*., **36(15)**: 2711-2721.

30. Khun, K.K., Mahajan, A. and Bedi, R.K. (2011). Surfactant Assisted Growth of Nanostructured Tin oxide films for gas sensing applications. *Electron. Mater. Lett*., **7(4)**: 303-308.

31. Jalilpour, M. and Fathalilou, M. (2012). Effect of aging time and calcination temperature on the cerium oxide nanoparticles synthesis via reverse co-precipitation method. *Int. J. Phys. Sci*., **7(6)**: 944-948.

32. Chelliah, M., Rayappan, J.B.B. and Krishnan, U.M. (2012). Synthesis and characterization of cerium oxide nanoparticles by hydroxide mediated approach. *J. App. Sci*., **12**: 1734-1737.

33. Tas, A.C., Majewski, P. J. and Aldinger, F. (2000). Chemical preparation of pure and strontium and/or magnesium-doped lanthanum gallate powders. *J. Am. Ceram. Soc.*, **83(12)**: 2954-2960.

34. Jasmine Ketzial, J. and Nesaraj,S. A. (2011). Synthesis of CeO_2 nanoparticles by chemical precipitation and the effect of a surfactant on the distribution of particle sizes. *J. Ceram. Process. Res*., **12(1)**: 74-79.